

Journal of Materials Chemistry A

Materials for energy and sustainability

Accepted Manuscript

This article can be cited before page numbers have been issued, to do this please use: Q. Liu, Y. Li, Y. Fan, C. Su and G. Li, *J. Mater. Chem. A*, 2020, DOI: 10.1039/D0TA01845G.



This is an Accepted Manuscript, which has been through the Royal Society of Chemistry peer review process and has been accepted for publication.

Accepted Manuscripts are published online shortly after acceptance, before technical editing, formatting and proof reading. Using this free service, authors can make their results available to the community, in citable form, before we publish the edited article. We will replace this Accepted Manuscript with the edited and formatted Advance Article as soon as it is available.

You can find more information about Accepted Manuscripts in the [Information for Authors](#).

Please note that technical editing may introduce minor changes to the text and/or graphics, which may alter content. The journal's standard [Terms & Conditions](#) and the [Ethical guidelines](#) still apply. In no event shall the Royal Society of Chemistry be held responsible for any errors or omissions in this Accepted Manuscript or any consequences arising from the use of any information it contains.

PAPER

Chemoselective hydrogenation of α , β -unsaturated aldehyde over Rh nanoclusters confined in metal-organic framework †

Received 00th February 20xx,
Accepted 00th February 20xx

DOI: 10.1039/x0xx00000x

Qinglin Liu,^a Yinle Li,^a Yanan Fan,^a Cheng-Yong Su^a and Guangqin Li^{*a}

Selective hydrogenation of α , β -unsaturated aldehyde to achieve high selectivity towards a desirable product is still a great challenge, mainly because of the complex conjugate system. Herein, Rh nanoclusters encapsulated in MIL-101 (Cr), synthesized by double solvents method, are able to selectively hydrogenate C=C of α , β -unsaturated aldehyde cinnamaldehyde and achieve over 98% selectivity with conversion of 98% to saturated aldehyde in mild condition. The Fourier transform infrared spectroscopy confirms that MIL-101 acts as aldehyde protector to suppress the reactivity of C=O, and the X-ray photoelectron spectroscopy (XPS) data indicates that the electropositive Rh, owing to the electron transfer from Rh to MIL-101, preferentially absorbs C=C rather than C=O leading to improvement of the selectivity of saturated aldehyde. In addition, Rh@MIL-101 can also efficiently hydrodefluorinate of aryl fluoride with good stability. This work gives out a basic strategy to develop other selective heterogeneous catalysts *via* structure modulation for synergetic catalysis.

Introduction

To hydrogenate α , β -unsaturated aldehyde towards high yields of saturated aldehyde or unsaturated alcohol is significantly important for industrial manufacture, such as petrochemicals, pharmaceuticals and perfume.¹⁻⁴ Because the complex conjugate system including two active functional groups of C=C and C=O, it is difficult to accurately crack only one functional conjugate bond.⁵⁻⁸ Cinnamaldehyde (CAL), a classical α , β -unsaturated aldehyde with both C=O bond and C=C bond, is a complex conjugated system. A great amount of noble metals based catalysts (such as Pt, Pd) for selective hydrogenation CAL to hydrocinnamaldehyde (HCAL) have been reported recently,⁹⁻¹⁴ however, the selectivity is usually lower than 90% over 1 MPa H₂ gas.¹⁵⁻¹⁷ Moreover, the hydrogenation of C=C or C=O is easily over hydrogenated to saturated alcohol.¹⁸⁻²⁰ Hence, to find out a kind of catalysts with a powerful ability to hydrogenate only C=C or C=O in the conjugated compounds is still a great strategy. Although Rh-based catalyst applied for selective hydrogenation of α , β -unsaturated aldehydes is rarely reported, it has been applied in unsaturated aldehydes hydrogenation, such as benzaldehyde, exhibiting excellent activity and selectivity towards saturated aldehyde.²¹⁻²⁵ Thus, it can be

speculated that Rh element may be a superior candidate for selective hydrogenation of α , β -unsaturated aldehydes.

Metal-organic frameworks (MOFs) are well-known for their large internal surface areas, stable chemical structure and appropriate size of pores.²⁶⁻³¹ Owing to these outstanding characteristics, MOFs have been attached great attention in heterogeneous catalysis, especially for compound combined MOFs with metal particles.³²⁻³⁶ Metal particles can be confined into MOFs, which will keep the metal from aggregating or losing for long durability with high activity.³⁷⁻⁴¹ In addition, the organic linkers or the metal nodes of MOFs can be a sort of Lewis acid site, which may accelerate the reaction process and improve the selectivity of the desired product.^{39, 41-44}

Herein, we report a highly efficient and chemoselective heterogeneous catalyst Rh@MIL-101 which has been prepared by double solvents method. The obtained Rh@MIL-101 exhibits excellent performance in selective hydrogenation of CAL with 98% conversion in 5 h and over 98% selectivity of HCAL, much better than commercial Rh/C and other M@MIL-101 (M=Pt, Pd), and maintains stable activity after 6 successive cycles. More importantly, the Lewis acid site from MIL-101 and significant C=C bond hydrogenation ability from Rh nanoclusters may promote the selective hydrogenation.

Experimental

Materials.

Chromic chloride hexahydrate (CrCl₃·6H₂O), terephthalic acid (H₂BDC), sodium hexachlororhodate (III) (Na₃RhCl₆), and sodium

^a MOE Laboratory of Bioinorganic and Synthetic Chemistry, Lehn Institute of Functional Materials, School of Chemistry, Sun Yat-Sen University, Guangzhou 510275, P. R. China. E-mail: liguangqin@mail.sysu.edu.cn.

† Electronic Supplementary Information (ESI) available. See DOI: 10.1039/x0xx00000x

borohydride (NaBH_4) were purchased from Aladdin (Shanghai, China). All the chemicals were used without any further purification.

Preparation of Rh@MIL-101.

The MIL-101 (Cr) was synthesized according to the literature reported before.⁵ Rh nanoclusters were confined within MIL-101 (Cr) by double solvents method. Briefly, 100 mg MIL-101 was dispersed in 20 mL of n-hexane, 180 μL deionized water containing 0.05 mmol Na_3RhCl_6 was added dropwise within 20 min, under vigorously stirring. After stirring for 3h, the solid powder was settled down in the bottom and then the supernatant was decanted, allowed the powder get dried in air at room temperature. The as-synthesis sample was further dried at 150 $^\circ\text{C}$ under vacuum for 10 h. After removing n-hexane and water in MIL-101, Rh ion was reduced by adding 5 mL 0.6 M NaBH_4 , after vigorously stirring for 30 min, the grey product was collected by centrifuging and washed by water for 3 times, and was dried at 60 $^\circ\text{C}$ under vacuum overnight.

Preparation of Rh nanoparticles.

Rh nanoparticles were synthesized by directly reduced using NaBH_4 as reductant. Briefly, 0.1 mmol Na_3RhCl_6 was dissolved in 5 mL water, 3 mmol NaBH_4 was added and stirred for 30min. The products were obtained after washing with double-distilled water for several times and dispersed in 1ml EtOH for further use.

Characterization.

The morphology and microstructure were tested by field-emission scanning electron microscopy (FESEM, SU8010, Hitachi) and transmission electron microscopy (TEM, JEM-1400 Plus, JEOL). High resolution images and element mappings were carried out on high-resolution transmission electron microscopy (HRTEM, ARM200P, JEOL). The crystalline structures of samples were characterized by powder X-ray diffraction (XRD, Rigaku, SmartLab), with Cu K α radiation under operation conditions of 40 kV and 30 mA. X-ray photoelectron spectroscopy (XPS) spectra were tested by a VG ESCALABMKII instrument. Fourier transform infrared (FT-IR) spectra were detected on Bruker Alpha spectrometer. Metal content of the catalysts was analyzed by inductively coupled plasma mass spectrometry (ICP-MS, Thermo Fisher Scientific). The N_2 adsorption-desorption isotherms were determined by Quantachrome Instruments Autosorb-iQ2-MP at 77K.

Chemoselective hydrogenation of cinnamaldehyde.

In a typical procedure, 5 mg catalyst was dispersed in 3 mL ethanol then 100 μL cinnamaldehyde (CAL) was added to the mixture in a high-pressure reaction glass vial. The glass vial was purged with pure H_2 for at least 3 time to remove the air, and eventually kept the H_2 pressure at 1 MPa. The reaction was carried out at desired time and temperature, and kept stirring with the speed of 600 rpm. After finishing the reaction, the solution was centrifuged and then analyzed by gas chromatography - mass spectrometry (GC-MS, SHIMAZU QP 2010) with a flame ionization detector (FID).

Hydrodefluorization of aryl chlorides.

View Article Online

DOI: 10.1039/D0TA01845G

0.1 mmol aryl chlorides and 10 mg catalyst were added to 5 mL water and kept ultrasound for 5 min to obtain a homogeneous solution before transferred into a 25 mL round-bottom flask. Removed the air in the round-bottom flask and then kept the final H_2 pressure at 0.1MPa using a H_2 balloon. After finishing the reaction, the solution was extracted by ethyl acetate and then analyzed by GC-MS.

Result and discussion

To produce Rh nanoclusters confined in metal-organic framework, MIL-101 (Cr) was firstly synthesized by the hydrothermal method as reported (Fig. S1 \dagger).^{2a} The double solvents method was adopted to prepare the Rh@MIL-101 catalyst, and morphology was analyzed by transmission electron microscopy (TEM). As shown in Fig. 1, Rh nanoclusters homogeneously dispersed in the MIL-101, with the mean diameter of 1.7 nm (Fig. 1a and Fig. S2 \dagger). The high resolution transmission electron microscopy (HRTEM) image showed the lattice fringe of 0.22 nm, which was corresponding to the (111) plane of Rh element (Fig. 1b). To test the element distribution of Rh@MIL-101, energy-dispersive X-ray spectroscopy (EDS) element mappings were carried out, and Rh element was distributed homogeneously in the entire MIL-101 (Fig. 1c). To confirm the structure of as-prepared materials, X-ray diffraction (XRD) was examined and shown in Fig. S3 \dagger . The obviously diffraction peaks of Rh@MIL-101 were corresponding to pristine MIL-101, no diffraction peaks from the structure of face-centered-cubic (fcc) Rh were observed, due to the low amount of Rh loading and ultrafine size of the particles, which was consistent with TEM images.^{39,45} The N_2 adsorption isotherms of MIL-101 and Rh@MIL-101 both showed a mixture of type I and IV curves (Fig. S4 \dagger). The Brunauer–Emmett–Teller (BET) surface area and total pore volume of MIL-101 were 3735 $\text{m}^2 \text{g}^{-1}$ and 1.63 $\text{cm}^3 \text{g}^{-1}$, respectively. Compared to pure MIL-101, the BET surface area and pore volume of Rh@MIL-101 decreased to 1715 $\text{m}^2 \text{g}^{-1}$ and 0.63 $\text{cm}^3 \text{g}^{-1}$, indicating that the cavities of MIL-101 were partially occupied by highly dispersed Rh nanoclusters.^{46,47} The Fourier transform infrared (FT-IR) spectrum of Rh@MIL-101 still preserved the characteristics of MIL-101 (Fig. S5 \dagger). The actual metal amount of catalyst was 4.4 wt%, confirmed by inductively coupled plasma mass spectrometry

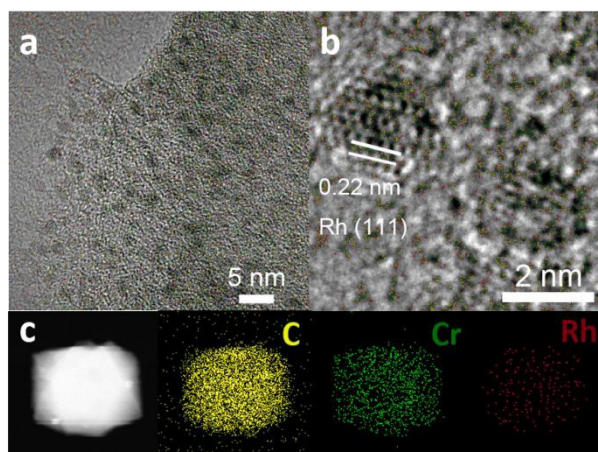


Fig. 1 (a) TEM image (b) HRTEM image and (c) HAADF-STEM-EDS element mappings of Rh@MIL-101.

(ICP-MS), listed in Table S1†. Taking account for the EDS mapping result, XRD and ICP-MS, Rh nanoclusters dispersed homogeneously in the MIL-101 have been successfully synthesized.

To investigate the activity and selectivity of α , β -unsaturated aldehydes hydrogenation, cinnamaldehyde was selected to evaluate the performance of Rh@MIL-101. Since both of the selectivity hydrogenation products, hydrocinnamaldehyde (HCAL) and cinnamyl alcohol (COL), are widely used as perfume or reaction intermediate, there is a great desire to develop catalysts with wonderful activity and selectivity, to solely hydrogenate C=O bond or C=C bond.⁴⁸⁻⁵¹ The hydrogenation reaction here was carried out in relatively mild conditions, and the results were displayed in Fig. 2. The schematic of CAL hydrogenation is shown in Fig. 2a, cinnamaldehyde is firstly hydrogenated to HCAL or COL, and sequentially experienced over hydrogenating to undesired product HCOL. Then, the impact of temperature towards the hydrogenation reaction was explored (Fig. 2b). The conversion could reach more than 98% with high selectivity from 30 °C to 90 °C, which means that the catalyst retains an impressive performance in a wide range of temperature. Hence, 30 °C was chosen as a proper temperature in the following tests. And the time-source hydrogenation reaction data (Fig. 2c) showed that the reaction conversion raised from 42% in first 0.5 h to 98% after 5 h, and the selectivity for HCAL kept in a high level (> 98%) in 5 h. When the reaction time was extended to 6 h, the selectivity was well remained, indicating the over hydrogenation hardly happened. Furthermore, reaction under different H₂ pressures was carried out (Fig. 2d). With increasing the gas pressure, reaction conversion raised rapidly, while the selectivity of HCAL was always

over 98%. This implies that Rh@MIL-101 could give out almost single hydrogenation product and avoid overhydrogenating.

For comparison, Pt@MIL-101, Pd@MIL-101 were synthesized by the same recipe, and the XRD patterns and morphology images had no significant difference with Rh@MIL-101 (Fig. S3 and S6†). Then, pure Rh nanoparticles were prepared by directly reduced using NaBH₄. Obviously, Rh nanoparticles with mean diameter of 5.7 nm were larger than Rh nanoclusters within MIL-101 from TEM image (Fig. S7†), further demonstrating the significance of confinement effects of the MIL-101. These four kinds of catalysts were performed CAL hydrogenation under the same condition as Rh@MIL-101, and the results were shown in Fig. 2e. Pt@MIL-101 showed the unsatisfied activity (55%) and the Pd@MIL-101 presented 92% conversion of CAL, but generated 27% of over hydrogenation product. As for commercial Rh/C, with the average particle size of 2.3 nm (Fig. S8†), merely achieved 53% of CAL conversion. Pure Rh NPs performed even worse (merely 20% conversion) in hydrogenation reaction, mainly due to the large size and severe aggregation. MIL-101 had less than 5% selectivity of HCAL, which could be thought as a negligible influence for Rh@MIL-101 hydrogenation reaction. The detailed catalysis results including turnover frequency (TOF) based on metal loading were calculated to evaluate intrinsic reactivity, and listed in the Table S2†. It should be noted that Rh@MIL-101 presented the best activity and selectivity compared to other noble metal catalysts and commercial Rh/C, indicating the support MIL-101 accelerated the reaction process and may act as active site for aldehyde protector to enhance HCAL selectivity.

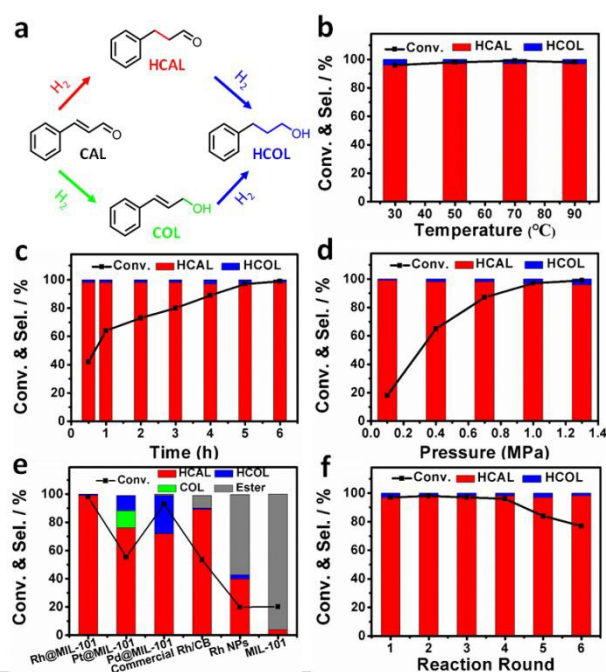


Fig. 2 (a) Schematic of CAL hydrogenation. (b) Activity and selectivity changes of Rh@MIL-101 for hydrogenation of CAL with different temperature after 5 h. (c) different time at 30 °C after 5 h and (d) different H₂ pressure after 5 h. (e) The activity and selectivity changes for hydrogenation of CAL with different catalysts after 5 h at 30 °C. (f) The stability test of Rh@MIL-101 for hydrogenation of CAL (reaction conditions: 100 μ L CAL, 5mg catalysts, 30 °C, 5 h, 1 MPa H₂).

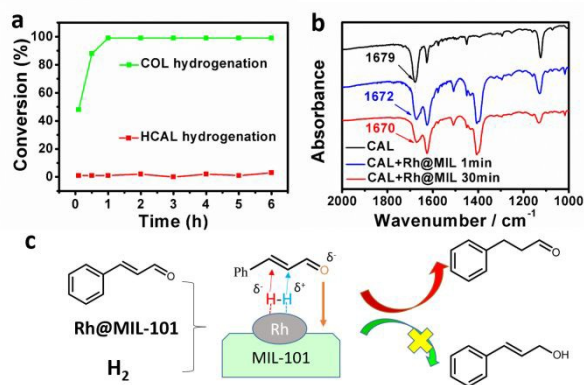


Fig. 3 (a) HCAL and COL hydrogenation performances of Rh@MIL-101. (b) FT-IR spectra of CAL adsorption on the Rh@MIL-101. (c) possible mechanism for CAL hydrogenation over Rh@MIL-101 with MIL-101 as aldehyde protector.

Recycle ability is necessary to be considered to fully evaluate the catalytic performance. Thereby the stability test of Rh@MIL-101 for selective hydrogenation was carried out. Even after 6 successive cycles of CAL hydrogenation reaction, Rh@MIL-101 still retained great activity and selectivity to HCAL, as shown in Fig. 2f. The structure and morphology of reused catalyst were detected to be maintained (Fig. S9†), indicating that MIL-101 kept the Rh nanoclusters from aggregation and presented the excellent catalytic performance and recycle ability.

To investigate the universality of Rh@MIL-101, different α , β -unsaturated aldehydes were hydrogenated to corresponding saturated aldehyde by Rh@MIL-101. As shown in Table 1, almost all the substrates can reach over 90% conversion within 6 h reaction, accompanied by high selectivity towards saturated aldehyde products. Due to the steric hindrance brought by ethyl, β -ethylcinnamaldehyde achieved only 80% conversion even after 12 h reaction, but still remained high selectivity for C=C bond hydrogenation product. It suggests that Rh@MIL-101 is an excellent catalyst for selective hydrogenation of α , β -unsaturated aldehydes.

To further understanding the reason for high selectivity of CAL hydrogenation over Rh@MIL-101, the COL and HCAL hydrogenation reactions were explored over Rh@MIL-101 (Fig. 3a). COL was completely hydrogenated to HCOL within 1 h. On the contrary, HCAL hardly converted to HCOL in the entire reaction, indicating that Rh@MIL-101 can actively transform CAL to HCAL, but inhibit C=O bond hydrogenation, leading to the high yield of HCAL.

Since the surface electronic property is related to the selectivity of catalyst to a great extent,⁵²⁻⁵⁵ the chemical state of Rh@MIL-101 was characterized by X-ray photoelectron spectroscopy (XPS). As shown in Fig. S10†, the strong peak at 307.5 eV and 312.1 eV were corresponding to Rh⁰ 3d_{5/2} and 3d_{3/2} of pure Rh NPs, respectively. After combining with MIL-101, the peak of Rh⁰ shifted to 307.9 eV and 312.5 eV. In addition, the peak of Cr 2p_{3/2} obviously shifted from 577.9 eV to 577.3 eV after immobilization of Rh NPs, indicating the electron transfer happened from Rh to MIL-101.^{56,57} Since C atom in the C=O is electropositive, electropositive Rh in MIL-101 may be able to absorb the C=C bond rather than C=O, result in the high selectivity towards HCAL.^{9,58}

To deeply explore the mechanism for selective hydrogenation, FT-IR was used to examine the adsorption of CAL on Rh@MIL-101. As

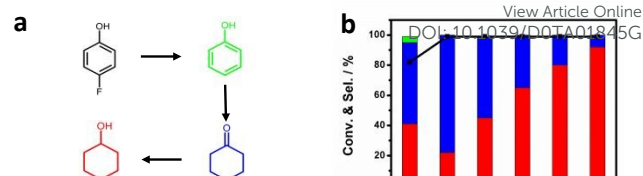


Table 1 Selective Hydrogenation of Different α , β -Unsaturated Aldehydes over Rh@MIL-101.^a

Entry	Substrate	Product	Time (h)	Conv. (%)	Sel. (%)
1			3	99	98
2			5	99	98
3			12	80	95
4			6	90	81
5			6	93	92
6			4	99	99

^a Reaction condition: α , β -unsaturated aldehydes (0.5 mmol), catalyst (5mg), Ethanol (3 mL), 30 °C, 1 MPa H₂, monitored by gas chromatography-mass spectrometry (GC-MS).

shown in Fig. 3b, the obvious C=O stretching vibration peak (1679 cm⁻¹) can be found in the spectra of pure CAL. When the catalyst Rh@MIL-101 was added and stirred for only 1min, the absorbance of C=O stretching vibration peak was severely weakened and the peak was red shift to 1672 cm⁻¹. After stirring for 30 min, it became much weaker and further red shift (1670 cm⁻¹), which may be attributed to interaction between the Lewis acid sites of MIL-101 and one of the oxygen lone pairs,^{5,59,60} as the similar adsorption behavior was found on the bare MIL-101 (Fig. S11†). The interaction between aldehyde group and MIL-101 inhibited the hydrogenation of C=O bond. This reveals that the synergistic effect of electropositive Rh nanoclusters and aldehyde protector MIL-101 is the key to avoid over hydrogenation and keeps high selectivity of saturated aldehyde.

Encouraged by these promising results, we believe that Rh@MIL-101 may be also a good candidate catalyst for other heterogeneous reaction. Here the catalytic activity of Rh@MIL-101 for the hydrodefluorination of aryl fluorides was further examined in mild condition. As shown in Fig. 4, p-fluorophenol was completely hydrodefluorinated within 30 min over Rh@MIL-101, and produced 92% of final product cyclohexanol after 90 min reaction. Rh@MIL-101 performed much better than other catalysts (Table S3†), and retained stable activity even after eight rounds of hydrodefluorination reaction (Fig. 4d and S12†). In addition, Rh@MIL-101 was also suitable for catalyzing some other aryl fluorides and presented excellent activity (Table S4†). In brief, Rh@MIL-101 is thought as an outstanding catalyst for hydrodefluorination, which would be benefit to degrade the excess fluorochemical in the environment.⁶¹⁻⁶²

Conclusions

To conclude, Rh nanoclusters confined with MIL-101 have been synthesized for selective hydrogenation of α , β -unsaturated aldehyde. Rh@MIL-101 presents excellent performance in selective hydrogenation of cinnamaldehyde with 98% conversion in 5 h and over 98% selectivity towards saturated aldehyde. Because Lewis acid of MIL-101 interacts with the C=O group, leading to the C=C bond more reactive and avoiding the aldehyde over hydrogenation. Moreover, the electropositive Rh, owing to electron transfer between Rh and MIL-101, prefers to react with C=C bond, further inhibits over hydrogenating. In addition, the structural synergy of Rh nanoclusters and MIL-101 not only promises the high selectivity of α , β -unsaturated aldehyde hydrogenation, but also performs great activity and stability in degrading different aryl fluoride in a mild condition. The obvious improvement of activity and selectivity by structural synergistic effect between electropositive Rh and aldehyde protector MIL-101 provides an effective method to design catalysts for selective hydrogenation.

Conflict of interest

The authors declare no conflict of interest.

Acknowledgements

This work was supported by National Key R&D Program of China (2018YFA0108300), High Level Talent of China and Guangdong Province, The 100 Talents Plan Foundation of Sun Yat-sen University, the Program for Guangdong Introducing Innovative and Entrepreneurial Teams (2017ZT07C069), and the NSFC Projects (21821003, 21890380).

Notes and references

- M. Poliakoff and P. Licence, *Nature*, 2007, **450**, 810.
- Y. Ren, Y. Tang, L. Zhang, X. Liu, L. Li, S. Miao, D. Sheng Su, A. Wang, J. Li and T. Zhang, *Nat. Commun.*, 2019, **10**, 4500.
- J. Zhang, L. D. Ellis, B. Wang, M. J. Dzara, C. Sievers, S. Pylypenko, E. Nikolla and J. W. Medlin, *Nat. Catal.*, 2018, **1**, 148-155.
- J. Zhang, B. Wang, E. Nikolla and J. W. Medlin, *Angew. Chem. Int. Ed.*, 2017, **56**, 6594-6598.
- M. Zhao, K. Yuan, Y. Wang, G. Li, J. Guo, L. Gu, W. Hu, H. Zhao, and Z. Tang, *Nature*, 2016, **539**, 76-80.
- M. Tamura, D. Yonezawa, T. Oshino, Y. Nakagawa and K. Tomishige, *ACS Catal.*, 2017, **7**, 5103-5111.
- Y. Nakagawa, K. Takada, M. Tamura and K. Tomishige, *ACS Catal.*, 2014, **4**, 2718-2726.
- L. O. Mark, N. Agrawal, A. M. Román, A. Holewinski, M. J. Janik and J. W. Medlin, *ACS Catal.*, 2019, **9**, 11360-11370.
- P. Wang, Q. Shao, X. Cui, X. Zhu and X. Huang, *Adv. Funct. Mater.*, 2018, **28**, 1705918.
- H. Liu, Z. Li and Y. Li, *Ind. Eng. Chem. Res.*, 2015, **54**, 1487-1497.
- W. Lin, H. Cheng, L. He, Y. Yu and F. Zhao, *J. Catal.*, 2013, **303**, 110-116.
- W. Sang, T. Zheng, Y. Wang, X. Li, X. Zhao, J. Zeng and J. G. Hou, *Nano Lett.*, 2014, **14**, 6666-6671.
- X. Yang, D. Chen, S. Liao, H. Song, Y. Li, Z. Fu and Y. Su, *J. Catal.*, 2012, **291**, 36-43.
- X. Zhang, Y. C. Guo, Z. C. Zhang, J. S. Gao and C. M. Xu, *J. Catal.*, 2012, **292**, 213-226.
- H. Gu, X. Xu, A. a. Chen, P. Ao and X. Yan, *Catal. Commun.*, 2013, **41**, 65-69.
- X. Han, R. Zhou, B. Yue and X. Zheng, *Catal. Lett.*, 2006, **109**, 157-161.
- X. Yuan, J. Zheng, Q. Zhang, S. Li, Y. Yang and J. Gong, *AIChE J.*, 2014, **60**, 3300-3311.
- S. M. Rogers, C. R. A. Catlow, C. E. Chan-Thaw, A. Chutia, N. Jian, R. E. Palmer, M. Perdjon, A. Thetford, N. Dimitratos, A. Villa and P. P. Wells, *ACS Catal.*, 2017, **7**, 2266-2274.
- Y. Long, S. Song, J. Li, L. Wu, Q. Wang, Y. Liu, R. Jin and H. Zhang, *ACS Catal.*, 2018, **8**, 8506-8512.
- X. Han, R. Zhou, B. Yue and X. Zheng, *Catal. Lett.*, 2006, **109**, 157-161.
- T. Harada, S. Ikeda, Y. H. Ng, T. Sakata, H. Mori, T. Torimoto and M. Matsumura, *Adv. Funct. Mater.*, 2008, **18**, 2190-2196.
- Y. Cao, M. Tang, M. Li, J. Deng, F. Xu, L. Xie and Y. Wang, *ACS Sustain. Chem. Eng.*, 2017, **5**, 9894-9902.
- D. J. M. Snelders, N. Yan, W. Gan, G. Laurency and P. J. Dyson, *ACS Catal.*, 2012, **2**, 201-207.
- M. Tamura, K. Tokonami, Y. Nakagawa and K. Tomishige, *ACS Catal.*, 2016, **6**, 3600-3609.
- M. Ibrahim, R. Poreddy, K. Philippot, A. Riisager and E. J. Garcia-Suarez, *Dalton Trans.*, 2016, **45**, 19368-19373.
- L. Chen, R. Luque and Y. Li, *Chem. Soc. Rev.*, 2017, **46**, 4614-4630.
- K. Shen, L. Zhang, X. Chen, L. Liu, D. Zhang, Y. Han, J. Chen, J. Long, R. Luque, Y. Li and B. Chen, *Science*, 2018, **359**, 206-210.
- K. Na, K. M. Choi, O. M. Yaghi and G. A. Somorjai, *Nano Lett.*, 2014, **14**, 5979-5983.
- S. Dissegna, K. Epp, W. R. Heinz, G. Kieslich and R. A. Fischer, *Adv. Mater.*, 2018, **30**, 1704501.
- K. Jayaramulu, F. Geyer, M. Petr, R. Zboril, D. Vollmer and R. A. Fischer, *Adv. Mater.*, 2017, **29**, 1605307.
- R. Medishetty, L. Nemeč, V. Nalla, S. Henke, M. Samoć, K. Reuter and R. A. Fischer, *Angew. Chem. Int. Ed.*, 2017, **129**, 14938-14943.
- H. Liu, L. Chang, L. Chen and Y. Li, *J. Mater. Chem. A*, 2015, **3**, 8028-8033.
- M. Rivera-Torrente, M. Filez, R. Hardian, E. Reynolds, B. Seoane, M. V. Coulet, F. E. Oropeza Palacio, J. P. Hofmann, R. A. Fischer, A. L. Goodwin, P. L. Llewellyn and B. M. Weckhuysen, *Chem.-Eur. J.*, 2018, **24**, 7498-7506.
- C. Rosler, S. Dissegna, V. L. Rechac, M. Kauer, P. Guo, S. Turner, K. Ollegott, H. Kobayashi, T. Yamamoto, D. Peeters, Y. Wang, S. Matsumura, G. Van Tendeloo, H. Kitagawa, M. Muhler, I. X. F. X. Llabres and R. A. Fischer, *Chem.-Eur. J.*, 2017, **23**, 3583-3594.
- J. Cheng, X. Gu, P. Liu, T. Wang and H. Su, *Journal of Materials Chemistry A*, 2016, **4**, 16645-16652.
- J. Song, X. Gu, J. Cheng, N. Fan, H. Zhang and H. Su, *Applied*

- Catalysis B: Environmental*, 2018, **225**, 424-432.
- 37 H. Zhang, M. Huang, J. Wen, Y. Li, A. Li, L. Zhang, A. M. Ali and Y. Li, *Chem. Commun.*, 2019, **55**, 4699-4702.
- 38 L. Chang and Y. Li, *Mol. Catal.*, 2017, **433**, 77-83.
- 39 X. Li, B. Zhang, L. Tang, T. W. Goh, S. Qi, A. Volkov, Y. Pei, Z. Qi, C. K. Tsung, L. Stanley and W. Huang, *Angew. Chem. Int. Ed.*, 2017, **56**, 16371-16375.
- 40 X. Gu, Z. H. Lu, H. L. Jiang, T. Akita and Q. Xu, *J. Am. Chem. Soc.*, 2011, **133**, 11822-11825.
- 41 Y. Z. Chen, Y. X. Zhou, H. Wang, J. Lu, T. Uchida, Q. Xu, S. H. Yu and H. L. Jiang, *ACS Catal.*, 2015, **5**, 2062-2069.
- 42 X. Chen, K. Shen, D. Ding, J. Chen, T. Fan, R. Wu and Y. Li, *ACS Catal.*, 2018, **8**, 10641-10648.
- 43 X. Li, Z. Guo, C. Xiao, T. W. Goh, D. Tesfagaber and W. Huang, *ACS Catal.*, 2014, **4**, 3490-3497.
- 44 X. Li, T. W. Goh, L. Li, C. Xiao, Z. Guo, X. C. Zeng and W. Huang, *ACS Catal.*, 2016, **6**, 3461-3468.
- 45 A. Aijaz, A. Karkamkar, Y. J. Choi, N. Tsumori, E. Ronnebro, T. Autrey, H. Shioyama and Q. Xu, *J. Am. Chem. Soc.*, 2012, **134**, 13926-13929.
- 46 Z. Guo, C. Xiao, R. V. Maligal-Ganesh, L. Zhou, T. W. Goh, X. Li, D. Tesfagaber, A. Thiel and W. Huang, *ACS Catal.*, 2014, **4**, 1340-1348.
- 47 Q. L. Zhu, J. Li and Q. Xu, *J. Am. Chem. Soc.*, 2013, **135**, 10210-10213.
- 48 K. R. Kahsar, D. K. Schwartz and J. W. Medlin, *J. Am. Chem. Soc.*, 2014, **136**, 520-526.
- 49 S. Bai, L. Bu, Q. Shao, X. Zhu and X. Huang, *J. Am. Chem. Soc.*, 2018, **140**, 8384-8387.
- 50 H. Liu, L. Chang, L. Chen and Y. Li, *ChemCatChem*, 2016, **8**, 946-951.
- 51 K. Yuan, T. Song, D. Wang, X. Zhang, X. Gao, Y. Zou, H. Dong, Z. Tang and W. Hu, *Angew. Chem. Int. Ed.*, 2018, **57**, 5708-5713.
- 52 J. Zhang, Z. Gao, S. Wang, G. Wang, X. Gao, B. Zhang, S. Xing, S. Zhao and Y. Qin, *Nat. Commun.*, 2019, **10**, 4166.
- 53 L. Lin, S. Yao, R. Gao, X. Liang, Q. Yu, Y. Deng, J. Liu, M. Peng, Z. Jiang, S. Li, Y. W. Li, X. D. Wen, W. Zhou and D. Ma, *Nature Nanotech.*, 2019, **14**, 354-361.
- 54 J. Jiao, R. Lin, S. Liu, W. C. Cheong, C. Zhang, Z. Chen, Y. Pan, J. Tang, K. Wu, S. F. Hung, H. M. Chen, L. Zheng, Q. Lu, X. Yang, B. Xu, H. Xiao, J. Li, D. Wang, Q. Peng, C. Chen and Y. Li, *Nature Chem.*, 2019, **11**, 222-228.
- 55 S. Yoshimaru, M. Sadakiyo, A. Staykov, K. Kato and M. Yamauchi, *Chem. Commun.*, 2017, **53**, 6720-6723.
- 56 M. Mukoyoshi, H. Kobayashi, K. Kusada, M. Hayashi, T. Yamada, M. Maesato, J. M. Taylor, Y. Kubota, K. Kato, M. Takata, T. Yamamoto, S. Matsumura and H. Kitagawa, *Chem. Commun.*, 2015, **51**, 12463-12466.
- 57 N. Ogiwara, H. Kobayashi, P. Concepcion, F. Rey and H. Kitagawa, *Angew. Chem. Int. Ed.*, 2019, **58**, 11731-11736.
- 58 D. F. and S. P., *J. Catal.*, 1995, **152**, 217-236.
- 59 M. Chen, N. Maeda, A. Baiker and J. Huang, *ACS Catal.*, 2012, **2**, 2007-2013.
- 60 H. Wang, S. Bai, Y. Pi, Q. Shao, Y. Tan and X. Huang, *ACS Catal.*, 2018, **9**, 154-159.
- 61 R. Baumgartner and K. McNeill, *Environ. Sci. Technol.*, 2012, **46**, 10199-10205.
- 62 D. Huang, G. A. de Vera, C. Chu, Q. Zhu, E. Stavitski, J. Mao, H. Xin, J. A. Spies, C. A. Schmuttenmaer, J. Niu, G. L. Haller and J. H. Kim, *ACS Catal.*, 2018, **8**, 9353-9358.